This paper was presented as invited lecture at the Fourteenth Meeting "New Trends in Fatigue and Fracture" (NT2F14) Belgrade, Serbia, 15–18 September, 2014

Sanja Z. Petronić

TRANSPARENT LAYER INFLUENCE ON MICROSTRUCTURAL CHANGES OF NIMONIC 263 IN LASER SHOCK PEENING PROCESSING

UTICAJ TRANSPARENTNOG SLOJA NA PROMENE U MIKROSTRUKTURI NIMONIC 263 LEGURE TOKOM MEHANIČKE OBRADE LASEROM

Originalni naučni rad / Original scientific paper
UDK /UDC: 620.187:669.245`26
Rad primljen / Paper received: 25.09.2014

Adresa autora / Author's address:
University of Belgrade, Faculty of Mechanical Engineering – Innovation Centre, contact: spetronic@mas.bg.ac.rs

Keywords
- laser shock peening
- superalloy
- SEM
- EDS
- profilometry
- microhardness

Ključne reči
- mehanička obrada laserom
- superlegura
- SEM
- EDS
- profilometrija
- mikrotvrdoća

Abstract

Laser shock peening (LSP) is one of the promising surface treatments for improving the fatigue, corrosion, wear resistance and hardness of the material. In this paper, LSP is applied on the Nimonic 263 superalloy surface. The changes in microstructure and in surface topography are observed and analysed by SEM, profilometer and microhardness tester. LSP is carried out with and without transparent layer, with the aim to investigate the influence of the transparent layer on microstructural changes. In this paper, the optimal process parameters are determined. Also, it is shown that the laser processing of the material in the presence of the transparent layer results in a more favourable microstructure and surface topography compared to the laser treatment without the transparent layer.

Izvod

Mehanička obrada laserom je jedna od vodećih površinskih obrada u cilju poboljšanja otpornosti na zamor, koroziju i habanje, kao i tvrdoću materijala. U ovom radu, mehanička obrada laserom je primenjena na površinu superlegure Nimonic 263. Promene u mikrostrukturi i površinskoj topografiji su praćene i analizirane skenirajućim elektronskim mikroskopom, profilometrom i merenjem mikrotvrdoće. Parametri laserskog procesa su varirani, a proces je izveden sa i bez transparentnog sloja u cilju analize uticaja transparentnog sloja na mikrostrukturne promene. U radu su određeni optimalni parametri procesa, i pokazano je da mehanička obrada laserom sa primenom transparentnog sloja daje povoljniju mikrostrukturu i površinske karakteristike u odnosu na obradu bez transparentnog sloja.

INTRODUCTION

Nickel based superalloys are commonly used in gas turbines, combustion chambers, casings, liners, exhaust ductings, bearing housings and other systems, /1/. They are designed to withstand conditions in harsh environments (high pressure and temperature) by thermomechanical treatments, /2, 3/.

Nimonic alloy 263 is an important precipitation hardening nickel-base superalloy, with high creep strength and oxidation resistance, good corrosion resistance, optimal thermal properties, strength coupled with ductility, wear and fatigue resistance.

Since the components of this alloy are primarily degraded by creep damage together with the harsh environment, it is necessary to retard the intergranular cracking and propagation for better performance at elevated temperatures and pressure.

Laser shock peening (LSP) is an innovative surface treatment technique which is successfully applied to improve fatigue performance of metallic components.

Depending on the laser processing parameters and their influence on the material the applied laser surface treatment during LSP can be considered as thermomechanical or mechanical, /4/. In the laser thermomechanical treatment (LTMT), upon the exposition to the beam, the material spot surface suffers changes due to heat influence (i.e. melting). On the other hand, laser mechanical treatment (LMT) of materials involves non-thermal changes; both the structure and properties of the material are changed by laser-induced shock waves. Introduced residual stresses affect the fatigue resistance, /5-7/, microhardness /8, 9/ and grain size, /10/.

In this work, the LSP processing of Nimonic 263 with and without the transparent layer is applied. Samples are exposed to the laser beam of different pulse duration values, energy density and fluence. The microstructure and

surface topography of laser peened areas are analysed and discussed.

Among many parameters that characterize surface topography, average surface roughness is still one of the most important, as are the fatigue and corrosion resistance and creep life, /11, 12/. In this paper, together with the average surface roughness, the following parameters are calculated and discussed: average maximum profile valley depth and average maximum profile peak height. Special attention is paid to the influence of transparent material on the microstructure. It is shown that the implementation of LSP together with controlled variation of process parameters (fluence, exposition time) as well as presence of transparent material affects the grain size, surface characteristics, microstructure, microhardness and the whole appearance of treated areas.

EXPERIMENT

Research has been carried out on nickel based superalloy Nimonic 263 sheets. The sheets are cold rolled and heat-treated in two stages: (1) solid solution at 1150°C, hold for 1 h and cooled rapidly in water, and (2) precipitation-treated at 800°C, hold for 8 h and then air-cooled. In order to produce samples that are to be subjected to laser irradiation, the sheets are cut in the form of plates with dimensions of 150×150×0.7 mm. The chemical composition is determined by gravimetric analysis.

Surface treatment is performed by Nd^{3+}:YAG laser type SWP 5002. Laser specifications are: wavelength 1064 nm, mean laser power 50 W (max.), pulse peak power 6 kW, pulse energy up to 100 J (max.), pulse duration 0.5–50 ms, pulse repetition rate 0.5–10 Hz, focal diameter 0.2–2 mm.

The diffuse reflectance spectra have been recorded by Labsphere RSA-PE-20 diffuse reflectance and transmittance accessory, which fits into the sample compartment of the Perkin Elmer Lambda 35 UV-VIS spectrometer.

Samples are coated with an absorptive-protective layer, a black paint. The first group of coated samples has been placed in a container with distilled water (a transparent layer) and exposed to the pulsed laser beam.

The second group of coated samples is exposed to the pulsed laser beam without the transparent layer. During the experiment, specific values of controllable laser parameters (voltage, focus, …) are chosen for each irradiation which has yielded specific values of beam parameters at the target (energy density, fluence). The controllable laser parameters used in this experiment are as follows: voltages of 200, 234 and 250 V; pulse durations of 0.6, 0.7 and 0.8 ms and focus -in positions 1, 2 and 3.

The damages generated by the laser beam have been observed by scanning electron and light microscopes and analysed by electro-dispersive spectrometry with the JEOL JSM/5800 scanning electron microscope (SEM) as the implemented device. Both the circularity and the grain size of the damages are measured by using the Autocad 2009 programme and the grain size is calculated by the circle method, /11/. The changes in the surface morphology of the irradiated samples have been determined by the Talystep profilometer and the Zygo NewView 7100 noncontact profilometer. Surface parameters (average roughness, average maximum profile valley depth, average maximum profile peak height and skewness) are calculated according to ISO 4287-1997 standard. The microhardness tests have been performed by Vickers using the Hauser 249A semi-automatic tester.

RESULTS AND DISCUSSION

The chemical composition of the samples is determined by gravimetric analysis and the results are given in Table 1.

Table 1. Chemical composition of Nimonic 263 superalloy (wt %).
Tabela 1. Hemijski sastav superlegure Nimonic 263 (tež. %)

C	Al	Si	Ti	Cr	Mn	Fe	Co	Mo	Ni
11.03	0.5	0.3	2.2	20	0.5	0.5	20	5.9	bal.

Reflectance measurements have been performed for both the Nimonic 263 surface and the Nimonic 263 surface covered with absorptive layer (Fig. 1). Results at 1064 nm show that after applying the absorptive layer the reflectivity has significantly dropped from 50.2% to 9.8%.

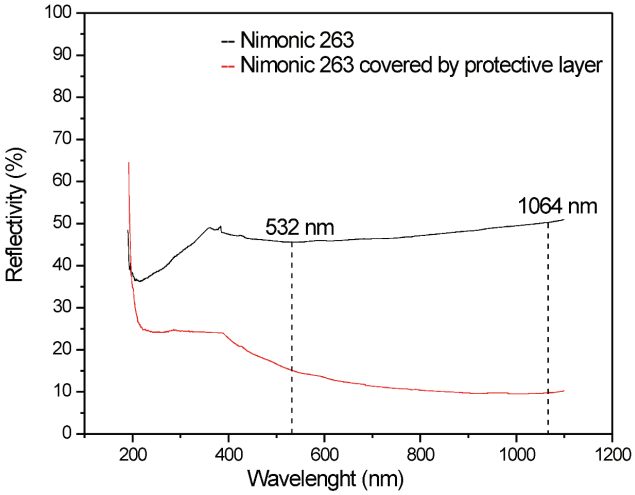

Figure 1. Comparative reflectance spectra of Nimonic 263 surface with and without protective paint.
Slika 1. Uporedni pregled spektra reflektanse površine Nimonic 263 sa i bez zaštitnog premaza

The protective overlay is used to absorb the incident heat and protect the metal target from the heat influence of the incident pulse.

Figure 2. shows the microstructures after direct ablation (laser thermomechanically treated material). The laser beam irradiates the surface of the material; the energy of the laser radiation together with the reflection of the material generate plasma. Consequently, the plasma causes a shock wave by its expansion.

The generation of shock waves can be realised by two different methods: with LMT process, and without LTMT transparent layer, /13/. During the laser thermomechanical treatment the plasma expands in the surrounding atmosphere. If a water, glass or quartz overlay is used (laser mechanical treatment), the plasma is trapped-like and its expansion in the surrounding atmosphere decreases. In this way, the pressure on the material is up to ten times higher. Also melting and material removal are reduced, /14/.

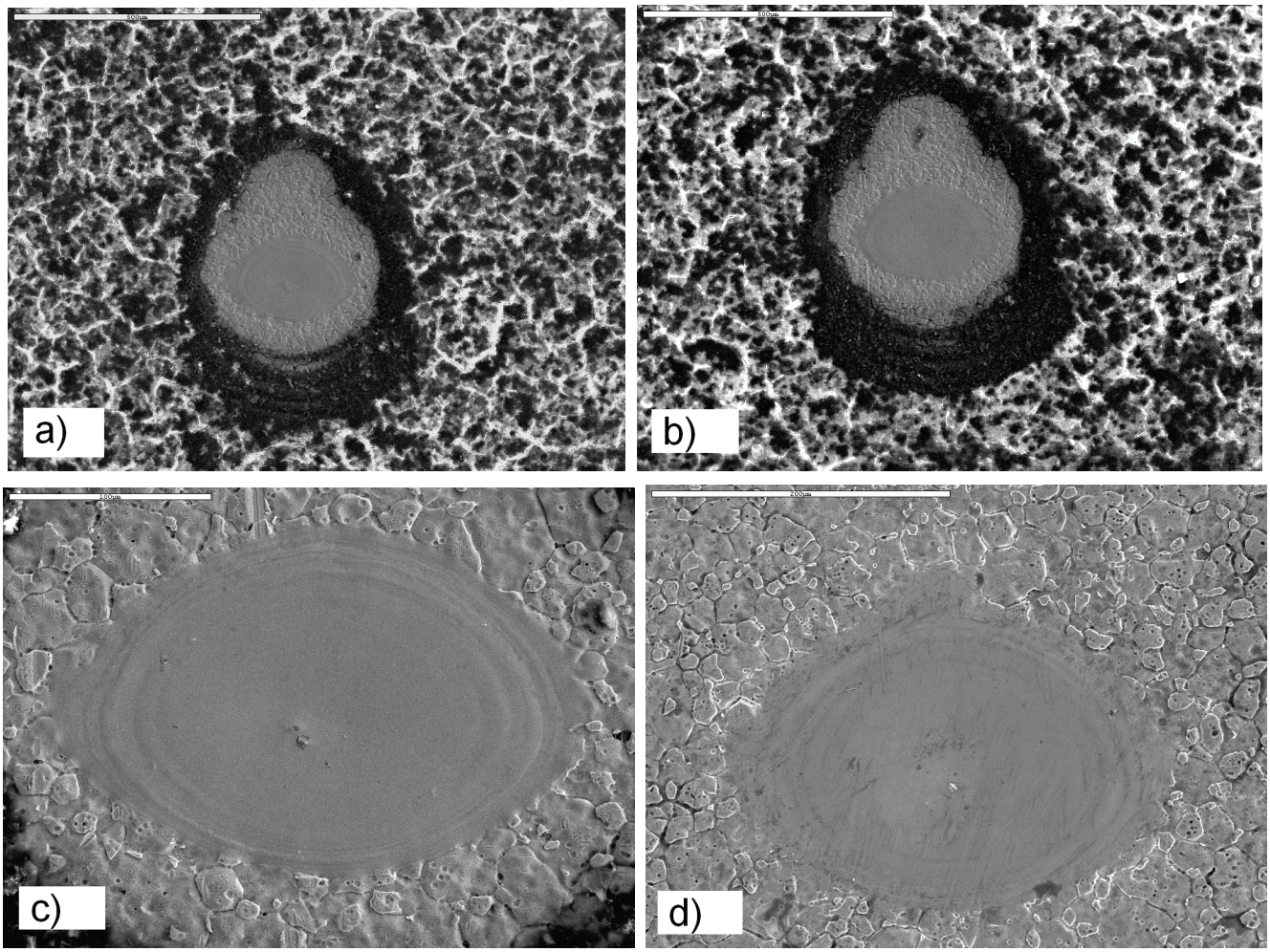

Figure 2. Laser beam interaction with black-coated material without transparent layer. Process parameters: a) pulse duration 0.6 ms, fluence 340 Jcm^{-2}, power density ~ 567 kWcm^{-2} (bar denotes 500 μm); b) pulse duration 0.7 ms, fluence 380 Jcm^{-2}, power density ~ 543 kWcm^{-2}, (bar denotes 500 μm); c) centre parts of damages presented in (a) (bar denotes 100 μm); d) centre parts of damages presented in (b) (bar denotes 200 μm).

Figure 2. Interakcija laserskog snopa sa crno premazanim materijalom bez transparentnog sloja. Parametri procesa: a) trajanje impulsa 0,6 ms, fluensa 340 Jcm^{-2}, gustina snage ~ 567 kWcm^{-2} (razmera linije 500 μm); b) trajanje impulsa 0,7 ms, fluensa 380 Jcm^{-2}, gustina snage ~ 543 kWcm^{-2}, (razmera linije 500 μm); c) središnji deo oštećenja prikazan pod (a) (razmera linije 100 μm); d) the središnji deo oštećenja prikazan pod (b) (razmera linije 200 μm)

Figures 2a-d show the surface damage after the LTMT. The processing parameters are set to values: pulse duration 0.6 ms, fluence 340 Jcm^{-2}, power density ~ 567 kWcm^{-2} (Fig. 2a); pulse duration 0.7 ms, fluence 380 Jcm^{-2}, power density ~ 543 kWcm^{-2} (Fig. 2b). By visual observation the two different areas could be noticed: re-melted material in the central part of the damage and the mechanically treated area around the melted circle. The re-melted material occurs in the centre of the spot where the pulse energy is the highest.

The re-melted parts, basically, follow the shape of the whole spot and are located in the centre where the highest pulse energy is applied. However, their shapes are quite irregular which depends largely on the homogeneity of the material and geometric characteristics of the sample. Since the material has been immersed in water, the cooling rate is very high and leads to quenching. Nevertheless the water evaporates at the spot (it flows to the spot from other areas). This process is very fast and as a result we can see metallic glass of very high hardness at the surface. A major influence on the shape of the re-melted part is from the onrush of water, its speed and the smoothness of arrival. In the fused parts, the grain boundaries are not visible; they do not follow the shape of the initial microstructure. A study of the re-melted part has revealed that grain boundaries loom up on its rims under the re-melted pool which confirms that the molten pool is cone-shaped and that the maximum amount of molten material is in the centre which corresponds to the laser beam mode.

Figures 3a and 3b show the microconstintuents observed in Fig. 2c. Secondary phases are formed due to specific features of laser treatment – rapid melting and solidification of materials, that is, high rates of heating and cooling of the material.

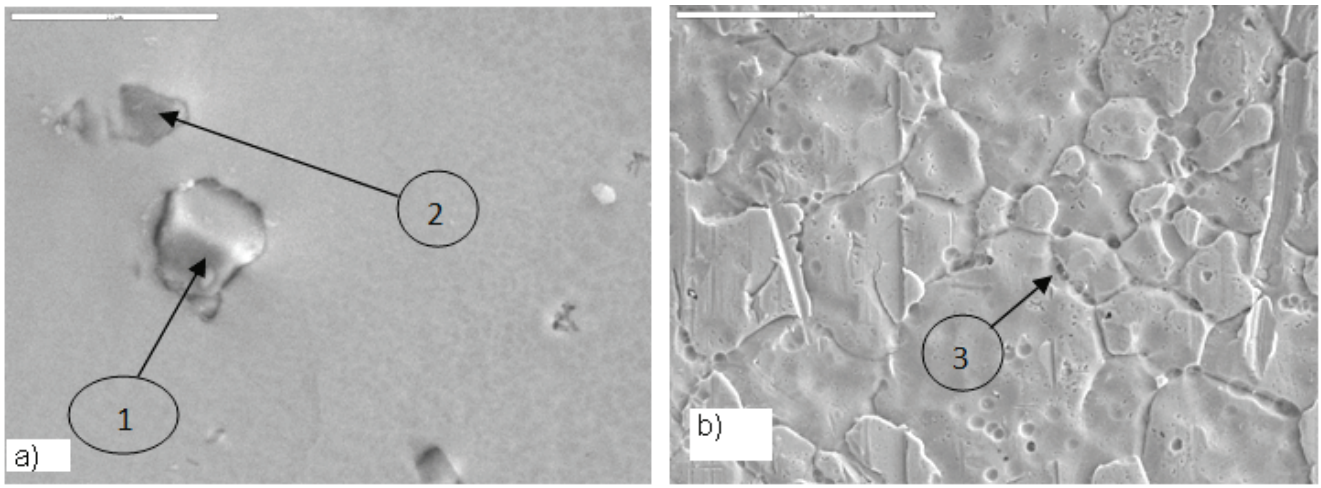

Figure 3. Microstructure observed in Fig. 2c: a) central, re-melted part (bar denotes 10 μm); b) area of mechanical treatment (bar denotes 50 μm).
Slika 3. Mikrostruktura uočena na sl. 2c: a) središnji, ponovo rastopljeni deo (razmera linije 10 μm); b) oblast mehaničke obrade (razmera linije 50 μm)

Table 2 presents EDS results taken at locations denoted in Fig. 3. The high content of Ti and C suggests that Ti carbides had formed. The size and morphology of these carbides are unfavourable and the locations of their occurrences are suitable for initial crack formation. The size of the microconstituents formed during the treatment of coated material without the transparent layer is larger than during the treatment with the transparent layer due to the longer cooling time and smaller pressure. The results of the EDS analysis presented in Table 2 suggest that in spectra 1 and 2 (in Fig. 3a) the carbides of Ti had segregated. The oxides might be the initiators of cracks, but for the applied laser parameters they have not initiated any cracks – no cracks were observed. We do not consider them as favourable for the cause of non-homogeneity and weakening of the microstructure because of their lower microhardness values compared to the base material.

Table 2. Results of EDS analysis in spots 1–3 in Fig. 3 (%wt).
Tabela 2. Rezultati EDS analize u tačkama 1–3 na sl. 3 (% tež)

El	EDS 1	EDS 2	EDS 3
O			9.28
C	11.03	7.07	
Al	0.18	0.43	2.33
Si	0.21	0.26	0.51
Ti	68.05	37.17	0.77
Cr	4.40	11.54	15.57
Mn			0.55
Fe			0.40
Co	3.83	10.57	18.52
Ni	9.35	25.80	47.02
Mo	2.97	4.24	5.05

The characterization of surface topography of mechanical work pieces with intricate shapes presents a significant challenge.

The surface morphology is an important aspect for the performance and life of parts of various machines. Cracks nucleate at positions where plastic strain concentrations are high. High surface roughness generates local stress concentration and accelerates crack initiation. For wear resistance applications, removal of the roughened surface is necessary, /16/. That is why a significant part of this research is dedicated to the surface roughness analysis.

As an illustration, Fig. 4 shows surface profiles of areas after LTMT with parameters: pulse duration 0.7 ms, fluence 380 Jcm^{-2}, power density ~ 543 kW cm^{-2}. The images are taken after the removal of the black paint.

The characteristics of the base material, calculated by the Gwyddion software are: average roughness 1.287 μm, average maximum roughness valley depth 3.766 μm, average maximum roughness peak height 3.317 μm, skewness |0.163|. The calculated characteristics of the material treated with the pulse duration 0.7 ms, fluence 380 Jcm^{-2}, power density ~ 543 kWcm^{-2}) are: average roughness 0.394 μm, average maximum roughness valley depth 1.123 μm, average maximum roughness peak height 1.043 μm, skewness |0.201|.

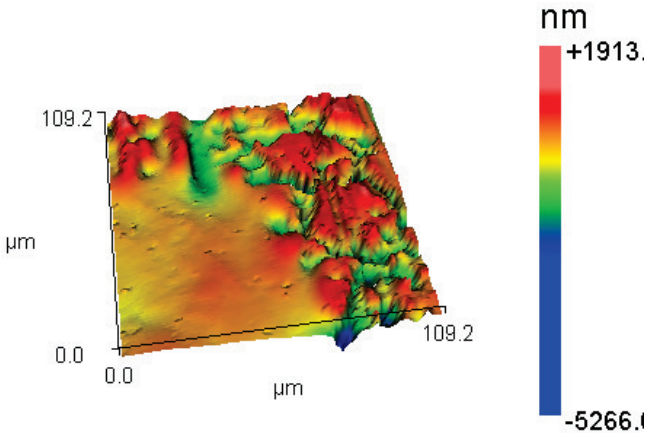

Figure 4. Surface profile taken by Zigo NewView 7100 profilometer. Laser treatment parameters of the surface: pulse duration 0.7 ms, fluence 380 Jcm^{-2}, power density ~ 543 kWcm^{-2}.
Slika 4. Profil površine dobijen sa Zigo NewView 7100 profilometrom. Parametri laserske obrade površine: trajanje impulsa 0,7 ms, fluensa 380 Jcm^{-2}, gustina snage ~ 543 kWcm^{-2}

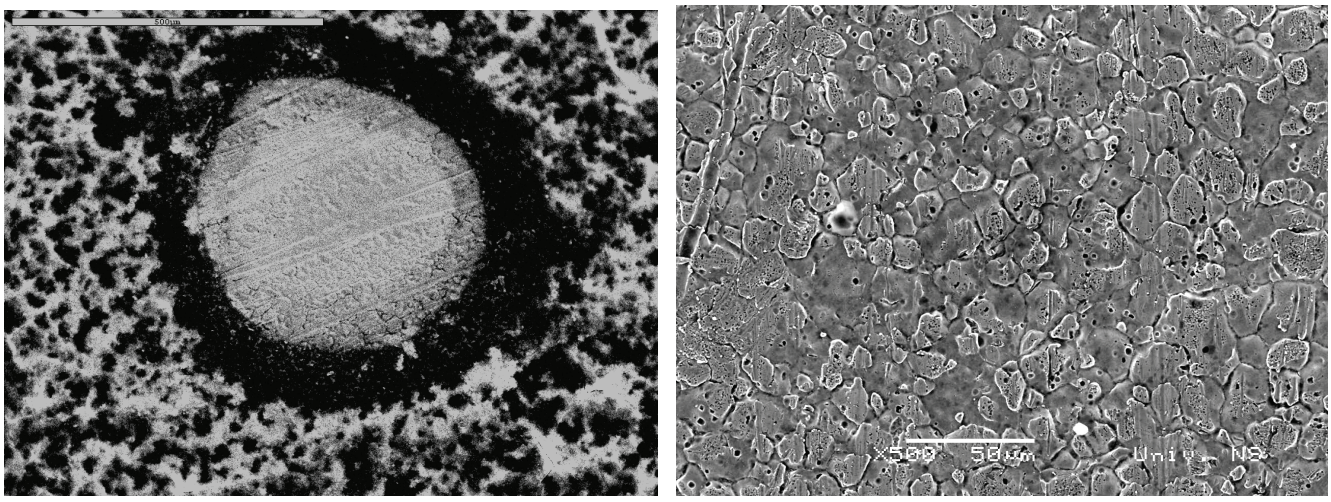

Figure 5. a) Microstructure developed after LMT (pulse duration 0.7 ms, energy density 333 Jcm^{-2}). The bar in the left upper corner denotes 500 μm; b) detail taken from Figure 5a.
Slika 5. a) Mikrostruktura nastala posle LMT (trajanje impulsa 0.7 ms, gustina energije 333 Jcm^{-2}). Razmera u gornjem levom uglu jeste 500 μm; b) detalj sa slike 5a

It can be noticed that the surface has an improved cleanness with a more regular structure and smaller grains compared to the structure of untreated surface.

Average maximum roughness valley depth and peak height have higher values than the average roughness which is due to the laser induced periods.

Figure 5 shows the microstructure obtained by LSP using the transparent layer. Because the transparent overlay prevents the laser-generated plasma from expanding rapidly away from the surface, an increase in shock wave intensity can be achieved. The transparent overlay results in more of the laser energy being delivered into the material as a shock wave than without it, /14/.

The hydrodynamic expansion of the generated plasma creates a high amplitude, short duration, pressure pulse due to the transparent layer which traps the plasma and does not allow its expansion into the surrounding atmosphere. As a result, shock waves are created, propagating into the metal. When the stress of the shock wave exceeds the dynamic yield strength of the metal, plastic deformation occurs, which consequently modifies the near-surface microstructure and properties, /17/.

EDS analysis is performed for the microstructure in Fig. 5. The EDS can reveal microstructural changes indirectly by comparing EDS spectra of the non-irradiated area with the spectra of the irradiated area. Secondary phases that develop after laser treatment with a protective layer are: alumina oxides, titanium carbides, and most of them can be considerable and favourable according to their size, morphology and location of formation. In LSP with the transparent layer, the melting did not occur.

In the mechanically treated area, calculated characteristics of the material treated with a fluence of ~ 567 $kWcm^{-2}$ (340 Jcm^{-2}, 0.6 ms, Fig. 5a) are: average roughness 0.451 μm, average maximum roughness valley depth 2.192 μm, average maximum roughness peak height 1.162 μm.

Pulse duration has the greatest impact, the higher the pulse duration the lower is the average roughness, and increasing the pulse energy density increases the average roughness. Also, the craters are observed in the LTMT of high pulse energy density.

The results show that laser treatment reduces the surface roughness, and in some cases generates a positive effect on the mechanical properties of materials.

The implementation of the transparent layer increases the plasma pressure by a trapping-like effect on the plasma expansion.

Mechanical treatment by laser which has required the absorbent coating – black and transparent material, gave the most favourable structure in the presence of distilled water.

Microhardness is measured by Vickers. The results for the base metal are 305 HV, for the surface after LMT are 345 HV, and for the surface after the LTMT are 368 HV. Different laser surface treatment parameters do not play an important role for microhardness values. However, it can be concluded that the LSP increases microhardness, as well as that microhardness values obtained in the LTMT are higher than those obtained by the LMT. This is explained by rapid melting and consequently rapid solidification of materials.

CONCLUSION

In this paper the two laser treatments, LTMT and LMT, have been applied to Nimonic 263 superalloy with various pulse energy densities, pulse durations and focus positions, with and without the transparent layer. Different outcomes have been noticed: as opposed to the LMT, the LTMT has created cracks due to higher power density of the laser beam and formation of unwanted secondary phases. LSP with transparent layer mostly produces favourable phases, while during the LSP process without the transparent layer, some unwanted phases have occurred. However, the higher microhardness is obtained in the process without the transparent layer. The treatment improved the surface cleanness – the structure became more regular and the size of the grains has decreased. After the laser treatment without the transparent material, the laser induced periods are noticed. The laser processing of the material in the presence of the transparent layer produced a better microstructure.

ACKNOWLEDGEMENTS

The work is supported by the Ministry of Education and Science of the Republic of Serbia, project TR35040.

REFERENCES

1. Fecht H., Furrer D., *Processing of Nickel-Base Superalloys for Turbine Engine Disc Applications*, Advanced Engineering Materials, (2000), 12 (2):.777-787.
2. Strondl, A., Milenkovic, S., Schneider, A., Klement, U., Frommeyer,G., *Effect of Processing on Microstructure and Physical Properties of Three Nickel-Based Superalloys with Different Hardening Mechanisms*, Adv. Engng. Mater., (2012) 14: 427-434.
3. Rösler, J., Götting, M., Genovese, D. Del , Böttger, B., Kopp, R., Wolske, M., Schubert, F., Penkalla, H.-J., Seliga, T., Thoma, A., Scholz, A., Berger, C., *Wrought Ni-Base Superalloys for Steam Turbine Applications beyond 700°C*, Adv. Engng. Mater., (2003) 5: 469-476.
4. Peyre, P., Carboni, C., Forget, P., Beranger, G., Lemaitre, C., Stuart, D., *Influence of thermal and mechanical surface modifications induced by laser shock processing on the initiation of corrosion pits in 316L stainless steel*, J Mater. Sci., (2007), 42 : 6866.
5. Heckenberger, U.C., Hombergsmeier, E., Holzinger, V., von Bestenbostel, W., *Advances in Laser Shock Peening theory and practice around the world: present solutions and future challenges*, Int. J Struct. Integrity, (2011), 2 (22).
6. Ballard, P., Fournier, J., Fabbro, R., Frelat, J., *Residual stresses induced by laser-shocks*, J Physique IV, C3 (1991), p.487.
7. Brockman, R.A., Braisted, W.R., Olson, S.E., Tenaglia, R.D., Clauer, A.H., Langer, K., Shepard, M.J., *Prediction and characterization of residual stresses from laser shock peening*, Int. J Fatigue, (2012), 36, p.96.
8. Lim, H., Kim, P., Jeong, H., Jeong, S., *Enhancement of abrasion and corrosion resistance of duplex stainless steel by laser shock peening*, J Mater. Process. Tech., (2012), 212, p.1347.
9. Tani, G., Orazi, L., Fortunato, A., Ascari, A., Campana, G., *Warm Laser Shock Peening: New developments and process optimization*, CIRP Ann. Manuf. Tech., (2011), 60, p.219.
10. Petronić, S., Kovačević, A.G., Milosavljević, A., Sedmak, A., *Microstructural changes of Nimonic 263 superalloy caused by laser beam action*, Phys. Scripta (2012), T149, p.014080.
11. Schumann, H., Metallographie, 13. neu bearbeitete Auflage, Deutscher Verlag für Grundstoffindustrie, Stuttgart, Germany (1994).
12. Fabbro, R., Peyre, P., Berthe, L ., Scherpereel, X., *Physics and applications of laser-shock processing*, Laser Appl. (1998), 10, p.265.
13. Schulze Niehoff, H., Vollertsen, F., *Laser induced shock waves in deformation processing*, J of Metallurgy (2005), 13 (3): 183-195.
14. Montross, C., Wei, T., Ye, L., Clark, G., Mai, Y., *Laser shock processing and its effects on microstructure and properties of metal alloys: a review*, Int. J of Fatigue, (2002), 10 (10): 1021-1036.
15. Ding, K., Ye, L., Laser Shock Peening, Performance and Process Simulation, Woodhead Publishing Ltd., Cambridge, UK (2006), pp 34-39.
16. Sahaya Grinspan, A., Gnanamoorthy, R., *Surface modification by oil jet peening in Al alloys, AA6063-T6 and AA6061-T4 Part 2: Surface morphology, erosion, and mass loss*, Applied Surface Science (2006), 253, pp.997-1005.
17. Clauer, A.H., *Laser shock peening for fatigue resistance*, Proc. of Surface Performance of Titanium, Gregory J.K., Rack H.J. and Eylon D. (eds), TMS, Warrendale, PA. The Metal Society of AIME, (1996), pp.217-30.